1. Scientific Context

How clouds will respond to global warming, which is the essence of **cloud feedback, continues to be a leading source of uncertainty** in the two most recent Coupled Models Intercomparison Project (CMIP) generations (Bony and Dufresne, 2005; Caldwell et al., 2016; Zelinka et al., 2016, 2020). Such diverse behavior impedes our ability to project the magnitude of future climate change and associated impacts (Zelinka et al., 2020; Cadwell et al., 2016; (Vial et al., 2013). The simulated feedback from high-level clouds is somewhat less variable between models than that from low-level clouds and modestly contributes to the spread in intermodel equilibrium climate sensitivity (ECS; Sherwood et al., 2020). As a consequence, not much attention has been paid to constrain it with observations. However, a recent assessment under the auspices of the World Climate Research Program (WCRP) indicates that the best estimate of high-cloud feedback is relatively large – about the same amplitude as tropical low-cloud feedback – but more importantly, solely relies on climate model estimates (Sherwood et al., 2020, their section 3.3.1).

With global warming, high-level cloud tops are expected to rise, according to climate models (e.g., Ceppi et al., 2017; Cesana et al., 2017). Because this altitude increase is accompanied by warming of the troposphere, the outgoing longwave (LW) emission from high-level clouds is expected to hold steady while the LW surface emission increases from warming of the surface (Hartmann and Larson, 2002), and the combined effect is a positive feedback that further warms the surface (Zelinka and Hartmann, 2010). Consistent with that theory, the models robustly predict a positive LW cloud feedback from non-low clouds (altitude > 3 km or pressure < 680 hPa), mainly driven by changes in cloud altitude (Zelinka et al., 2016), which is referred to as high-cloud altitude feedback, while changes in amount and optical depth offset each other.

Climate models could be overestimating the LW cloud feedback. Using CALIPSO observations, CALIPSO-like ESM outputs and a novel technique to characterize LW cloud radiative effect (CRE) based on five lidar-derived cloud parameters (opaque cloud cover and altitude, thin cloud cover, altitude and emissivity), Vaillant de Guélis et al. (2018) estimated CALIPSO-observed and simulated short-term LW cloud feedbacks. They found that the CALIPSO-derived cloud altitude feedback is positive and dominates the short-term LW cloud feedback in a climate model, consistent with results using long-term LW cloud feedback in ESMs (e.g., Zelinka et al., 2016). However, in the observations, the contribution of the changes in cloud altitude to the short-term LW feedback is smaller than that from changes in the opaque cloud fraction. Their results suggest that LW positive cloud feedback could be overestimated in climate model projections because they underestimate the magnitude of the negative feedback from opaque clouds. Further analysis of the short-term LW cloud feedback by Cesana et al. (2021b), using the same CALIPSO observations but over both continents and oceans and for a longer record, corroborates that the main contributors to the short-term LW cloud feedback are changes in opaque cloud amount (negative feedback) and altitude (positive feedback) while the other components only modestly contribute. Yet, a multimodel assessment of the LW short-term feedback is lacking and should be undertaken in view of the availability of this new observational constraint.

The sign and magnitude of the shortwave (SW) feedback from non-low clouds remain highly uncertain and unconstrained. Unlike the LW cloud feedback, the SW cloud feedback from non-low clouds is typically negative, small, and more uncertain with values ranging from -

0.69 to 0.41 W m^2 K^{-1} in CMIP6 models (Figure 1b; e.g., Zelinka et al., 2016, 2020). Because the multimodel mean value of this feedback is relatively small (-0.08 and -0.09 W m^2 K^{-1} in CMIP5 and CMIP6 models, Figure 1b; e.g., Zelinka et al., 2016, 2020), it has received far less attention in the literature. However, its range of uncertainty is larger than that of low-cloud feedback and has increased compared to the previous CMIP generation (Figure 1b-e). A large part of that uncertainty is generated in the extratropics, where the SW feedback is mostly negative (Figure 1e). Cesana et al. (2021a) show that depending on the cloud phase representation and whether large precipitating ice particles (more specifically, stratiform snow) are accounted for in the radiation scheme or not, the SW cloud feedback from non-low clouds can contribute to nearly doubling the net cloud feedback in a climate model. Consistent with that result, they find that accounting for large ice particles in radiation schemes may also substantially affect the net cloud feedback of CMIP models. Additional observational constraint on middle- and high-level cloud feedbacks is therefore needed to further characterize the contribution of these clouds to climate change under global warming.

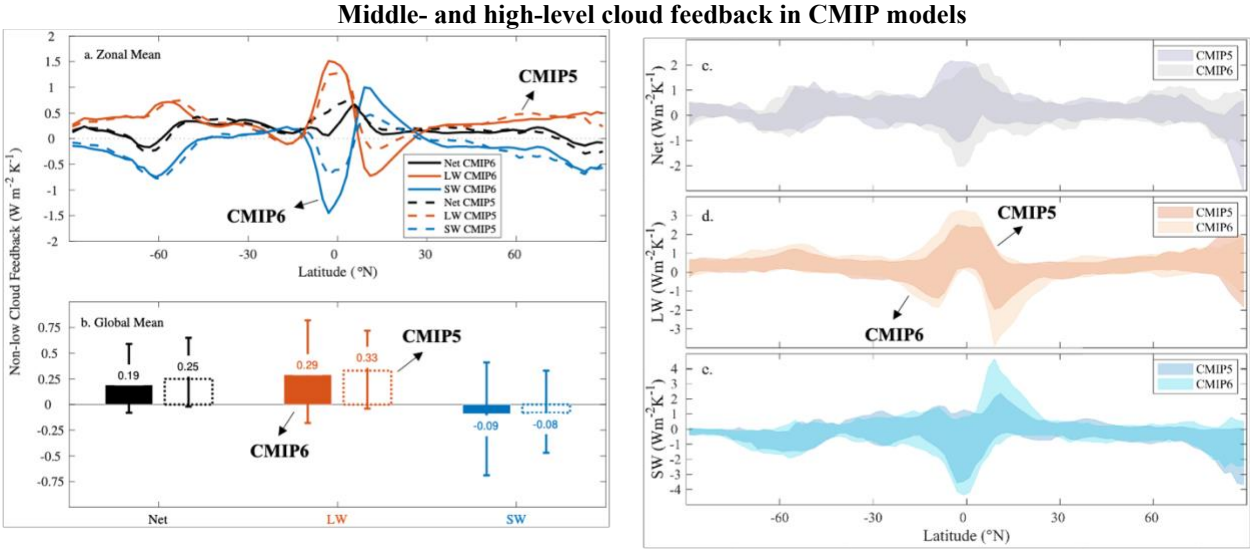

Figure 1: The middle- and high-level cloud feedback from CMIP6 and CMIP5 models remains highly variable (b). While the zonal mean of this cloud feedback is very similar in both generations, its regional magnitude (a) and spread (c-e) has increased in the CMIP6 generation. Cloud feedback computations from Zelinka et al. (2020) using 46 CMIP6 and 29 CMIP5 models.

CloudSat-CALIPSO observations could be used to infer cloud feedbacks from different cloud types. The synergistic use of lidar, radar and passive instruments onboard the A-Train satellite constellation makes it possible to better document cloud properties and quantify their associated radiative impacts, on a global scale (Hang et al., 2019; Kato et al., 2011; L'Ecuyer et al., 2019; Matus & L'Ecuyer, 2017). For example, optically thin cirrus clouds warm the system while optically thicker deep convective and multilayer clouds cool it (L'Ecuyer et al., 2019). In addition, these middle- and high-level clouds are driven by different cloud processes, and thus, there is no *a priori* reason to expect them to exhibit the same feedback in response to global warming (e.g., Bretherton, 2015; Cesana and Del Genio, 2021; Myers et al., 2021). Cesana and Del Genio (2021) showed that it is possible to infer cloud feedback for different cloud types from CloudSat-CALIPSO observations. They used CloudSat-CALIPSO observations in conjunction with reanalysis and complementary observations to determine the sensitivity of different cloud

types to the leading environmental factors. They further derived the cloud feedback for each cloud type by combining these sensitivities to the future changes of environmental factors, thereby providing much-needed direct constraints on stratocumulus and shallow cumulus cloud feedbacks. Assuming that middle- and high-level clouds are mainly driven by observable environmental factors, as hinted in the literature (e.g., Bony et al., 2016; Saint-Lu et al., 2020; Schiro et al., 2020; Zelinka and Hartmann, 2011), one could use the same method as Cesana and Del Genio (2021) to derive cloud feedbacks for different high-level cloud types observed by CloudSat-CALIPSO.

Problematic: In summary, the spread of middle- and high-level cloud feedback, which was already large CMIP5 models, has increased in CMIP6 models. The lack of observational constraint has made it difficult to evaluate their representation in climate models and impairs our confidence in the contribution of middle- and high-level clouds to future climate projections.

2. Objectives

Main objective: In the proposed work, we aim to determine the response of middle- and high-level clouds to climate variations, both on short and long-time scales (so-called short-term and long-term cloud feedbacks) from active-sensor CALIPSO-CloudSat observations – in conjunction with other A-Train observations – and develop constraints for climate models.

For this purpose, we will use CALIPSO-CloudSat datasets (e.g., 2B-CLDCLASS-LIDAR, CALIPSO-GOCCP, 2B-FLXHR-LIDAR), supported by additional satellite and reanalysis datasets (e.g., CERES, MODIS, MERRA-2), and a novel approach based on the sensitivity of clouds to environmental factors to infer feedbacks from different middle- and high-level cloud types (e.g., Cesana and Del Genio, 2021; Klein et al., 2017; Myers et al., 2021). Finally, we will apply our framework to NASA GISS-ModelE3 (Cesana et al., 2019a; Cesana et al., 2021a), exploiting its four configurations being submitted to CMIP6, as well as other CMIP6 models to place our results into a broader context. More specifically, we will undertake the following five activities:

1. Characterize the short-term feedbacks of middle- and high-level clouds from CloudSat-CALIPSO datasets (including vertical changes) in response to surface temperature forcings and their feedbacks.
2. Determine what environmental factors drive the variability of each middle- and high-level cloud type and further document the interannual changes (i.e., sensitivities) of these clouds in response to the leading environmental factors (e.g., surface temperature, upper-tropospheric stability, mid-tropospheric humidity, and large-scale vertical motion).
3. Building on results found above, infer the cloud feedback of each middle- and high-level cloud type assuming different possible scenarios of environmental factor future changes
4. Apply our framework to the four configurations of NASA GISS-ModelE3, which span a diversity of equilibrium climate sensitivity and cloud sensitivities to environmental factors, to constrain and better understand what drives changes in middle- and high-level cloud feedbacks.
5. Place our results into a broader context by assessing the middle- and high-level cloud feedbacks simulated by CMIP models and analyze the implications to ECS.

3. Proposed Activities

3.1. Characterizing the short-term cloud amount and radiative effect changes of each middle- and high-level cloud type

Since the simulated feedback from high-level clouds modestly contributes to the spread in intermodel climate sensitivity (Sherwood et al., 2020), less attention has been paid to constraining it and thus, observational constraints of middle- and high-level cloud feedback are still lacking. However, a recent study suggests this feedback may profoundly change the global net feedback (Cesana et al., 2021a). Additionally, the magnitude of the LW cloud feedback, mostly driven by middle- and high-level clouds, could be largely biased in climate models (Vaillant de Guélis et al., 2018). Finally, a growing body of literature has shown that different cloud types may be driven by distinct cloud processes, thereby exhibiting distinct cloud feedbacks (Figure 2; e.g., Cesana and Del Genio, 2021; Bretherton et al., 2015; Myers et al., 2021; Vaillant de Guélis et al., 2018).

Activity 1: We will separate characterize short-term contributions from different cloud types using existing CloudSat-CALIPSO datasets (e.g., CALIPSO-GOCCP OPAQ, 2B-CLDCLASS-LIDAR…).

We will use existing CloudSat-CALIPSO datasets to derive short-term cloud changes and cloud feedbacks from middle- and high-level clouds. To estimate these quantities, we will regress monthly anomalies of deseasonalized cloud fractions and cloud radiative effect fluxes against monthly anomalies of deseasonalized global mean surface temperatures using three different surface temperature datasets (Berkeley Earth Surface Temperature project, Rohde and Hausfather, 2020; NASA GISTEMP v4, (Lenssen et al., 2019); HadCRUT 4.6.0.0; Morice et al., 2012). We will pay particular attention to also estimate vertical changes of cloud fraction, when possible, which may sometimes reveal compensating changes from different altitudes that cannot be seen with traditional 2D cloud fractions (e.g., Cesana et al., 2019a).

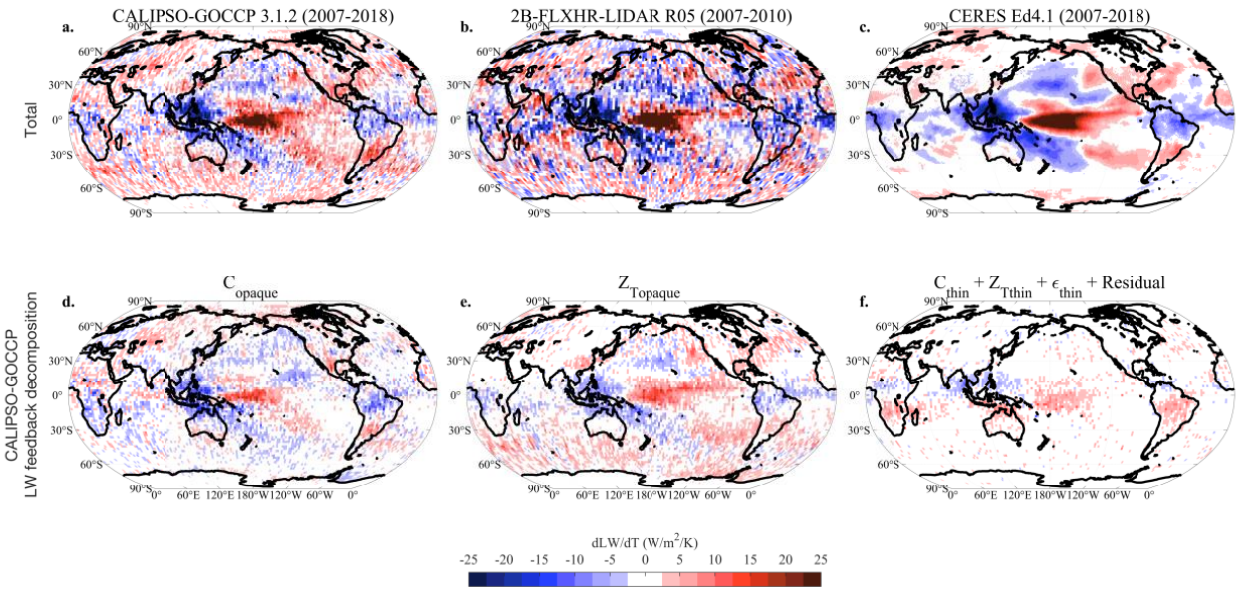

Figure 2:The short-term LW cloud feedback from all clouds that can be derived from top-of-Atmosphere radiative fluxes and surface temperature monthly anomalies (top) and further decomposed as a function of different cloud property contributions (bottom). Observations from (a) CALIPSO-GOCCP OPAQ (2007-2018; version 3.1.2), (b)

2B-FLXHR-LIDAR (2007-2010; version R05) and (c) CERES (2007-2018; version Ed4.1). Contributions from (d) opaque cloud cover, (e) opaque cloud altitude and (f) thin cloud cover, altitude, emissivity and the residual, all derived from CALIPSO-GOCCP OPAQ. The sum of (d-e-f) panels is equal to (a). Note that the contributions from opaque clouds (d, e) are far larger than that from thin clouds (f). From Cesana et al. (2021b).

The approach will be applied to two pairs of datasets (Table 1):

CloudSat-CALIPSO based datasets. The combined A-Train observations allow the distinction of radiative contributions from single-layer and multilayer clouds. For example, the 2B-CLDCLASS-LIDAR product R05 (Sassen and Wang, 2008; referred to as 2BCCL) merges collocated observations from the CloudSat CPR, CALIPSO lidar and MODIS spectroradiometer to classify clouds into eight types based on several criteria: their vertical and horizontal extent, precipitating state, temperature and radiance. Although eight cloud types are available in this dataset (deep convective, cirrus, nimbostratus, altostratus, altocumulus, cumulus including fair-weather and congestus, stratus and stratocumulus), we will only focus on the middle- and high-level cloud types (the first five of the list) and multilayer clouds. This latter type, which correspond to multiple non-contiguous cloudy layers in the same profile, has been shown to be ubiquitous and exert a strong influence on top-of-atmosphere (TOA) energy balance and atmospheric heating (e.g., L'Ecuyer et al., 2019; Hang et al., 2019). The corresponding SW and LW cloud radiative fluxes will be extracted from the collocated 2B-FLXHR-LIDAR Release 5 product (2BFL; Henderson et al., 2013; L'Ecuyer et al., 2008; Matus and L'Ecuyer, 2017). This product uses CloudSat, CALIPSO, and MODIS observations a forward radiative transfer model to derive estimates of radiative fluxes consistent with the cloud mask used in the 2BCCL dataset for the 2007-2010 period.

CALIPSO-CERES based datasets. The CALIPSO-GOCCP cloud phase observations (Cesana and Chepfer, 2013; Chepfer et al., 2010) provide 333 m-along-track-resolution near-nadir cloud profiles for 480 m height intervals. In the latest version of CALIPSO-GOCCP (version 3.1.2; Guzman et al., 2017), a new surface echo detection has been implemented (referred to as OPAQ), which allows discrimination of optically-thin clouds (surface-echo detected) from opaque clouds (no surface echo detected) and substantially reduces the biases in vertical cloud fraction from lidar attenuation (21.2% to 2.6% of false clear-sky detection). We will use this new diagnostic to discriminate thin from opaque middle- and high-level clouds. For the LW fluxes, we will follow the method introduced by Vaillant de Guélis et al. (2018), which uses five parameters derived from CALIPSO-GOCCP OPAQ to determine LW CRE at TOA: cloud altitude and cover from opaque and thin clouds separately as well as emissivity of thin clouds. Additionally, we will use Clouds and the Earth's Radiant Energy System (CERES) Energy Balanced and Filled (EBAF) (Loeb et al., 2018) observations for SW and LW CRE at TOA. Unlike the CloudSat-CALIPSO based datasets, CERES fluxes are not collocated with CALIPSO profiles, so we will not be able to estimate precisely the CRE of thin and opaque middle- and high-level clouds but rather the CRE of gridboxes in which either thin or opaque clouds dominate.

	CALIPSO-CERES		CloudSat-CALIPSO	
Product	GOCCP-OPAQ	CERES-EBAF	2B-CLDCLASS-LIDAR	2B-FLXHR-LIDAR
Short name	OPAQ	CERES	2BCCL	2BFL
Satellite	CALIPSO	CERES	CALIPSO-CloudSat-MODIS	CALIPSO-CloudSat-MODIS

Variables	Opaque and thin, middle- and high-level clouds,LW CRE	TOA and surface fluxes	5 middle- and high-level cloud types and multilayer clouds	TOA and surface fluxes
Time period	2007-2018	2007-2018	2007-2010	2007-2010

Table 1: We will use multiple CloudSat-CALIPSO datasets to characterize feedbacks of different types of middle- and high-level clouds.

3.2. Determining leading environmental factors of middle- and high-level cloud types and documenting their interannual changes

In recent years, several studies have shown that capturing the mechanisms that govern the change of clouds in response to environmental factor variations typical of climate warming is an essential condition — although not the only one — to predict future climate (e.g., Cesana and Del Genio, 2021; Myers et al., 2021; Scott et al., 2020; Klein et al., 2017). By doing such process-level analysis, one can better isolate climate model systematic biases in present day climate (e.g., Cesana et al., 2019a; Myers and Norris, 2015; Terai et al., 2016) and further infer cloud feedback by combining the sensitivities of clouds to environmental factors to the future changes of these environmental factors (e.g., Cesana and Del Genio, 2021; Myers et al., 2021; Klein et al., 2017).

Activity 2: We propose to determine the leading environmental factors of middle- and high-level cloud types and then further document their interannual variation (including any changes in vertical distribution).

To our knowledge, the relationship between middle- and high-level clouds and environmental factors have not been analyzed at a detail comparable to that for low-level clouds (e.g., Klein et al., 2017). However, some studies have already identified strong correlations between middle- and high-level clouds and observable environmental factors such as surface temperature, upper-tropospheric stability, large-scale vertical wind and mid-tropospheric humidity (Bony et al., 2016; Martins et al., 2011; Saint-Lu et al., 2019; Schiro et al., 2020; Zelinka et al., 2011). We will build on these results and further study the relationship between the aforementioned environmental factors and middle- and high-level cloud fraction using the same method as Cesana and Del Genio (2021) and Cesana et al (2019a) (see an example in Figure 3). For this purpose, we will compute 2D-histograms of environmental factors as a function of middle- and high-level cloud types and determine their correlation (Cesana and Del Genio, 2021, their Text S1 and Figure S1).

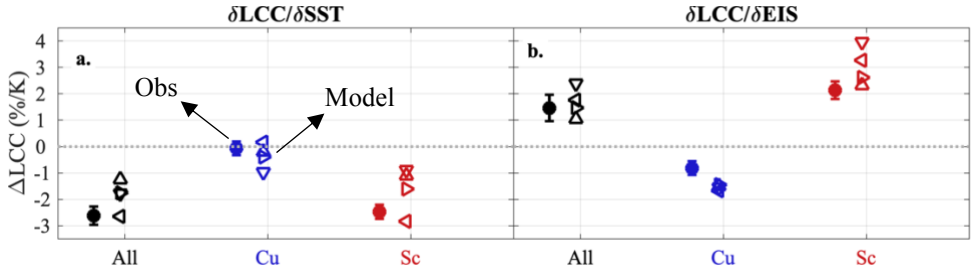

Figure 3: The observed and simulated sensitivities to environmental factors (SST on the left and EIS on the right) can be very different as a function of cloud types from CALIPSO-CASCCAD observations (solid circles, 2007-2016) and NASA GISS-ModelE3 simulations (empty triangles, 2007-2014), which confirms the need to breakdown the middle- and high-level clouds in cloud types. In this example (modified from Cesana and Del Genio, 2021), we use four configurations of GISS-ModelE3 (which is being submitted to CMIP) to emphasize the variability of the model

as a function of the choice of tuning parameters. We will use the same method for middle- and high-level cloud types with their leading environmental factors.

To calculate the interannual relationship between the cloud fraction of each middle- and high-level cloud type ($MHCF_{type}$) and the environmental factors (x), we will compute the monthly mean of $MHCF_{type}$ (and profiles) and regress them against monthly anomalies of environmental factors after having filtered out all columns with mean subsidence at 500 hPa ($\omega_{500} > 0$ hPa/day), typically dominated by low clouds. By doing so, we ensure that the cloud profiles, and therefore the TOA radiation, are dominated by middle- and high-level clouds. Since we expect multiple leading environmental factors, we will use multi-linear regression for the partial derivative (Figure 3) as in Cesana and Del Genio (2021) and Cesana et al. (2019a). This approach defines dynamically-based means and anomalies, as opposed to spatially-based anomaly/mean studies that focus on particular regions (e.g., McCoy et al., 2017; Qu et al., 2015). This technique will be applied to each middle- and high-level cloud type ($MHCF_{type}$) and to the opaque and thin cloud fractions. In addition, we will ensure that the sensitivities of $MHCF_{type}$ to environmental factors ($\partial MHCF_{type}/\partial x$) remain similar when adding or removing environmental factors to account for covariability. Finally, we will provide an uncertainty envelope for the observational estimates based on a diversity of reanalysis and observations (Figure 3; e.g., Cesana and Del Genio, 2021; Cesana et al., 2019a): NASA-MERRA2, ERSSTv5, HadISST1.1, NCEPv2, NOAA-CIRES-DOEv3 and ERA5.

3.3. Inferring middle- and high-level feedback for each cloud types

Because middle- and high-level clouds have not been identified as major contributors to CMIP model climate sensitivity, little attention has been paid to analyzing their cloud feedback. As a result, observation constraints for this feedback are lacking and our best estimate mostly relies on climate models (Sherwood et al., 2020).

Activity 3: We will infer feedbacks of middle- and high-level cloud types using a relatively new method (further described below) in concert with the CALIPSO, CloudSat-CALIPSO, CERES and other reanalysis and other global-scale satellite observations, which will provide a much-needed observation constraint for climate models.

To compute observationally infer cloud feedback, we first assume that the change in CRE in large-scale ascent regimes (as determined by the large-scale vertical wind at 500 hPa) is primarily driven by the change in MHCF as opposed to large-scale subsidence regimes in which low clouds prevail (Cesana et al., 2019a; Klein et al., 2017; Myers and Norris, 2016; Qu et al., 2014). Since this change in MHCF depends on the middle-and high-level cloud sensitivity to environmental factors described in Section 3.2 (i.e., the partial derivatives), we can therefore reconstruct the overall middle-and high-level cloud feedback using Eq. 1 and the sensitivity of CRE to MHCF to convert the MHCF change into a cloud feedback:

$$\frac{d\mathrm{CRE}}{dT} = \frac{d\mathrm{CRE}}{dMHCF} \sum_i \frac{\partial \mathrm{MHCF}}{\partial x_i} \frac{dx_\mathrm{i}}{dT} \qquad (1)$$

where the dCRE/dMHCF coefficient is the interannual CRE change with respect to MHCF obtained by linearly regressing monthly CRE anomalies from CERES-EBAF, GOCCP-OPAQ or the CloudSat-CALIPSO 2BFL combined products with the corresponding MHCF datasets

described in Table 1 (see also Cesana et al., 2019a and Cesana and Del Genio, 2021); dT is the global mean surface temperature anomaly;ˆand dx_i/dT can come from either a blend of reanalysis and observational datasets over the historical period (past few decades, e.g., Cesana and Del Genio, 2021) or from climate model simulations of the future climate (e.g., Cesana and Del Genio, 2021; Klein et al., 2017; Myers et al., 2021).

Since the partial derivatives of each cloud type with respect to their environmental factors can be different (Figure 3), we must further estimate the contribution of each cloud type separately in Eq. 1 and sum them (e.g., Cesana and Del Genio, 2021). Additionally, the partial derivatives of $MHCF_{type}$ with respect to their environmental factors vary depending on how frequently a cloud type is present in a gridbox (Cesana and Del Genio, 2021; their Figure S8). To represent the effect of each type of cloud depending on its relative presence in a given grid box, we normalize the partial derivatives of a cloud type by the sum of all cloud types in each grid box as in Eq. 2. To summarize, we will combine Eq. 2 and CALIPSO, CloudSat-CALIPSO and CERES observations (in blue below), reanalysis datasets (in purple below) with additional observational datasets and climate model outputs (in green below) to compute possible historical and future cloud feedback from middle- and high-level clouds.

$$\frac{d\mathrm{CRE}}{dT} = \sum_{type=1}^{j} \left[\frac{d\mathrm{CRE_{type}}}{d\mathrm{MHCF}_{type}} \left(\sum_i \frac{\partial \mathrm{MHCF_{type}}}{\partial x_i} \frac{dx_i}{dT} \right) \frac{\mathrm{MHCF_{type}}}{\mathrm{MHCF}} \right] \qquad (2)$$

OPAQ + CERES
2BCCL + 2BFL

OPAQ + reanalyses
2BCCL + reanalyses

OPAQ
2BCCL

Reanalyses/Observations (historical)
Climate model outputs (future)

3.4. Applying our framework to GISS-ModelE3 configurations to constrain and better understand middle- and high-level cloud feedbacks

As pointed out in the introduction, the lack of observational constraints for middle- and high-level cloud feedback has made it difficult to evaluate the fidelity of their response in climate models. Furthermore, their spread has increased in the most recent generation of CMIP models (Figure 1). Together, these problems limit our confidence in the contribution of middle- and high-level clouds to future climate projections.

Activity 4: We propose to build on the results from the previous activities to evaluate and better understand what drive middle- and high-level cloud feedback in climate models.

We will primarily analyze monthly outputs from global simulations of the four configurations of the latest version of the NASA GISS-ModelE version 3 Earth system model (ESM) (Cesana et al., 2019a; Cesana et al., 2021a), referred to as GISS-ModelE3. In three of the four GISS-ModelE3 configurations, only cloud-related parameters are varied and not parameterization formulations, while the last configuration also uses variant model physics formulations. They represent "equally-likely" physics representations that were primarily obtained by applying machine

learning methods to roughly 40 uncertain cloud-related parameters to optimize agreement with satellite observables (Elsaesser et al., in prep). The GISS modeling center uses these four configurations to represent a substantial diversity in their outcomes with cloud physics parameters and subsequent cloud and precipitation occurrences, and preliminary slab ocean simulations indicate that they span a sizable range of ECS (~3–4.5 K) both below and above the CMIP6 multimodel mean of 3.85 K (Cesana and Del Genio, 2021, using 40 models). This diversity is represented in both cloud sensitivities to environmental factors (Figure 3) and in the representation of middle- and high-level cloud feedbacks (Figure 4a-c) and high-level cloud fraction, which encompasses the observations almost everywhere (Figure 4d).

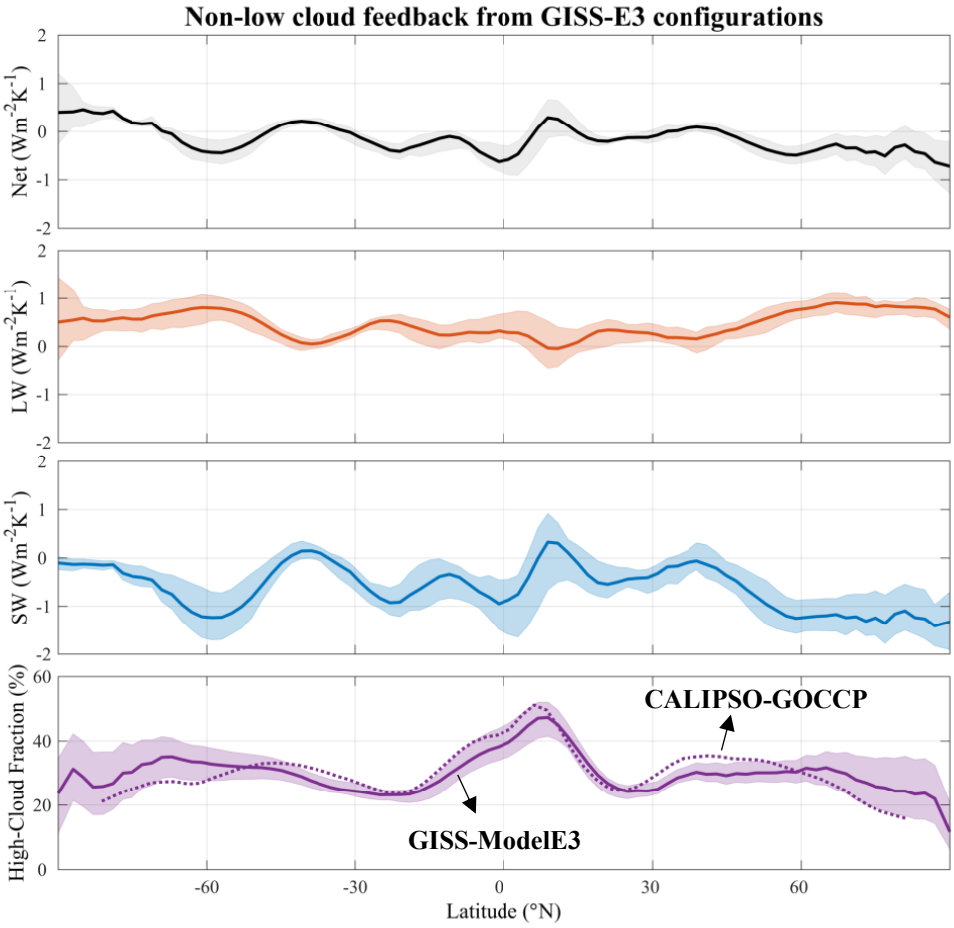

Figure 4: The mean net, LW and SW cloud feedbacks (a-c, solid lines) from four GISS-ModelE3 configurations, computed using the Zelinka et al. (2013) radiative kernels, show a substantial spread (shading) and reproduces part of the CMIP6 multimodel spread shown in Figure 1c-e. We also note that the CALIPSO-simulated GISS-ModelE3 high-level cloud fraction encompasses the CALIPSO-GOCCP high-level cloud fraction almost everywhere, suggesting that GISS-ModelE3 produce plausible high-level cloud fields, which it should as a result of the tuning process.

To ensure a fair evaluation that accounts for the observation limitations and uses similar cloud definitions and resolutions as in the observations, we will use the CALIPSO-like outputs from GISS-ModelE3, obtained through the use of the CALIPSO lidar simulator (Cesana and Chepfer, 2013), to compare with the CALIPSO-GOCCP observations. As part of synergistic project led by PI Cesana, the latest features of the lidar simulator, which are required to distinguish thin and opaque clouds, will be implemented in GISS-ModelE3. Therefore, we will be able to compute the same short-term (Activity 1) and inferred future (Activity 3) cloud feedbacks from thin and opaque clouds as well as the interannual variability of middle- and high-level clouds and covariability with leading environmental factors (Activity 2) and compare them against CALIPSO-GOCCP observations. Unfortunately, since no 2BCCL simulator or diagnostics are available at this point, we wil not be able to qualitatively compare these with climate model outputs. Additionally, we will compute the actual feedback (as opposed to inferred) for the middle- and high-level clouds to analyze possible

discrepancies between the inferred and actual feedbacks. For this purpose, we will use the pressure-optical depth cloud fraction from ISCCP simulator and the radiative kernels from Zelinka et al. (2013) as in Figure 4 with future scenarios consistent with those used in Activity 3 (either 4xCO_2 or uniform +4K increase).

Finally, we will also include the IPSL model in this analysis, which includes the necessary simulator outputs and a completely independent set of parametrizations. These will be provided by Helene Chepfer, a collaborator on this project.

Furthermore, by analyzing the different tuning parameter combinations of four GISS-ModelE3 configurations, we will be able to better pinpoint which tuning parameters affect each cloud type and their interannual variations and feedback in GISS-ModelE3. By doing so, we hope to understand the reasons for the diverse behavior of climate models with respect to middle- and high-level cloud feedback. For example, why some GISS-ModelE3 configuration can produce a positive SW feedback around 10˚N while another one produces a negative one (Figure 4) and which configuration is most likely correct according to the new observational constraints.

3.5. Assessing the middle- and high-level cloud feedback simulated by CMIP models and analyze the implications to ECS

As mentioned in the introduction (Section 1), the variation in model ECS is partly driven by variations in cloud feedbacks (e.g., Andrews et al., 2012; Bony and Dufresne, 2005; Caldwell et al., 2016; Qu et al., 2018; Vial et al., 2013). As a result, ECS estimates derived from models can be narrowed if cloud feedbacks are constrained by observations (e.g., Myers and Norris, 2016).

Activity 5: We will analyze the relationship between middle- and high-level cloud feedback and ECS uncertainty using GISS-ModelE3 configurations and additional CMIP models.

This activity will build on our previous results and on another funded effort led by PI Cesana, in which other GISS-ModelE3 configurations with different cloud-tuning parameters will be created, and their feedback computed. We will use this opportunity to analyze the effect of further cloud-parameter modifications on middle- and high-level cloud feedbacks, and ultimately on the ECS uncertainty, compared to the initial set of four GISS-ModelE3 configurations. We will compute the ECS of these configurations using the Gregory et al. (2004) method. Additionally, we will compute the contribution of each cloud feedback to ECS, following the method used in Vial et al. (2013) and Zelinka et al. (2020).

To place our results in a broader context, we will also analyze middle- and high-level cloud feedbacks from CMIP models and their link to ECS. As for GISS-ModelE3 and the IPSL model, we will use model outputs consistent with the observations, namely, the CALIPSO lidar simulator outputs. However, because the thin and opaque cloud fractions are not requested in the CMIP archive, we won't be able to evaluate the models against CALIPSO-GOCCP OPAQ thin and opaque cloud fractions. Instead, we will need to characterize the different middle-and high-level cloud regimes. For this purpose, we will exploit our results from Section 3.2, which describe the relationship of MHCF with environmental factors. Using a combination of environmental filters on cloud fraction can help separate cloud type regimes, such as shown by Cesana and Del Genio (2021) and Myers et al. (2021) with thresholds on EIS and ω_{500} to discriminate stratocumulus and

shallow cumulus. For example, we could use the CALIPSO lidar cloud fraction model outputs along with a simple threshold on ω_{500} to define regimes of strong tropical ascent (ω_{500} < -40 hPa/day; Figure 5 bottom left), typically deep convective clouds, and regimes of moderate tropical ascent (ω_{500} > -40 hPa/day; Figure 5 bottom right), typically middle- and high-level stratiform clouds. Therefore, we would be able to apply the same regime approach to the observations and use them to evaluate the models within our framework, e.g., short-term feedback (Activity 1), interannual variability (Activity 2) and "inferred" feedback (Activity 3). Finally, we will be able to further assess the contribution of middle- and high-level cloud feedback to ECS as a function of their level of performance against our observational constraint. By doing so, we intend to advance understanding of the cloud-climate feedback mechanisms related to middle- and high-level clouds, which remain poorly documented at this time.

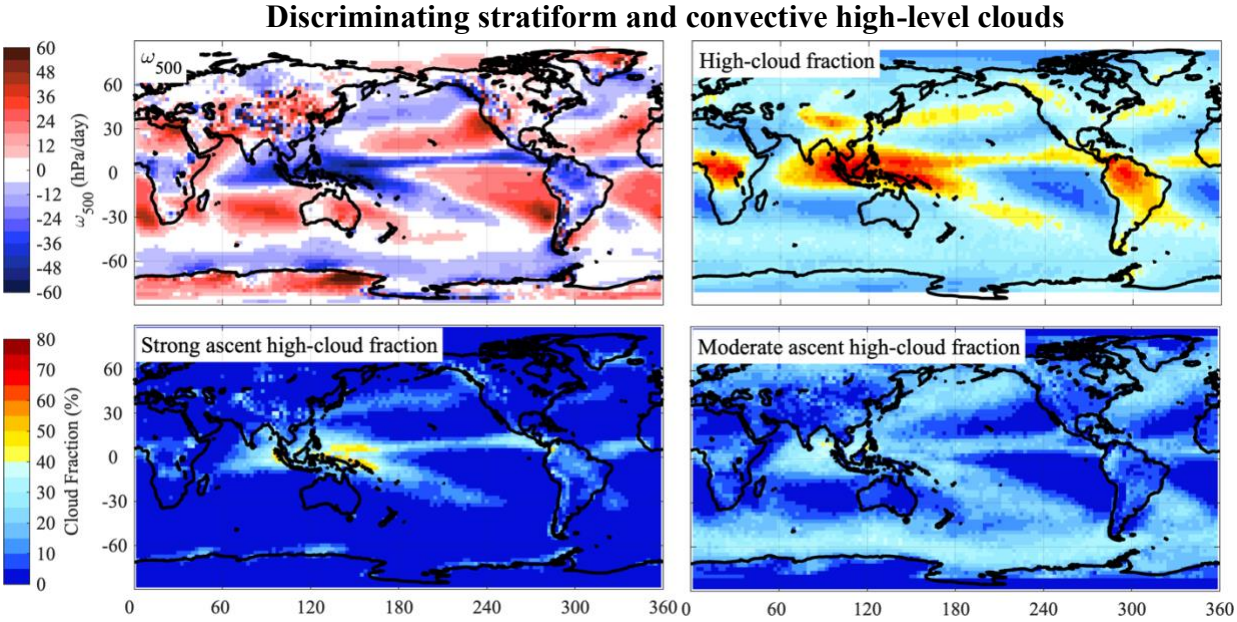

Figure 5:CALIPSO-GOCCP high-level cloud fraction (upper right) can be separated into strong (bottom left) and moderate ascent (bottom right) regimes using thresholds on ω_{500} (ω_{500} < -40 hPa/day and 0 > ω_{500} > -40 hPa/day, respectively). The observations are from CALIPSO-GOCCP (day and nighttime, 2007-2016) and a blend of reanalysis for ω_{500} (MERRA2, ERA5 and NCEP).

4. Work plan

4.1. Timeline

Year 1: We will characterize short-term contributions from different cloud types using CALIPSO-GOCCP OPAQ and CloudSat-CALIPSO datasets (Activity 1) as well as those from the two high-cloud regimes (strong and moderate ascent) for further climate model evaluation. As the observational constraints become available, we will begin the model evaluation (Activity 4 and 5).

Year 2: While finishing the model evaluation that uses Activity 1's results, we will also determine the leading environmental factors of middle- and high-level cloud types and then further document their interannual variation in the observations (Activity 2). In parallel, we will apply our framework to the climate models (Activity 4 and 5).

Year 3: Building on the results of Activity 2, we will infer feedbacks of middle- and high-level cloud types using the relatively new method described in Section 3.3 in concert with the CALIPSO, CloudSat-CALIPSO, CERES and other reanalysis and global-scale satellite observations (Activity 3). The resulting observational constraints will be used to evaluate the middle- and high-level cloud feedback in the models and to analyze and constrain the relationship between cloud feedback and ECS uncertainty using GISS-ModelE3 configurations and additional CMIP models (Activity 5).

We anticipate producing a total of at least four publications: one publication for Activity 1, 2 and 3, which includes the model evaluation describe in Activity 4, and another one for Activity 5.

4.2. Proposal Team

Dr. Gregory V. Cesana (PI, 0.36 total FTE over the 3-year period) is an expert on the use of CloudSat-CALIPSO observations and climate model evaluation of cloud-radiation properties and cloud feedbacks. He is the developer of Global-Climate Model (GCM)-oriented Cloud-Aerosol Lidar and Infrared Pathfinder Satellite Observation (CALIPSO) Cloud Product (GOCCP), the related cloud thermodynamic phase climatology product and the Cumulus and Stratocumulus CloudSat-CALIPSO Dataset (CASCCAD). Dr. Cesana also has experience in processing other CloudSat-CALIPSO level2 products into level3 datasets (2B-Geoprof-lidar, 2B-FLXHR-LIDAR and 2B-CLDCLASS-LIDAR). He will oversee all aspects of the proposed research. He will lead the different activities (1 to 5), which include estimating short-term cloud changes and feedbacks from middle- and high-level clouds, determining their main environmental factors, inferring their response to climate warming in the observations and using these results to evaluate the GISS and other CMIP models. He will dedicate more of his time in the final year to help inferring the cloud feedbacks and evaluating the models besides analyzing the relationship between cloud feedback and ECS in ESMs activities (3 to 5). Additionally, he will also be involved in the writing of the related publications and presenting the results in relevant conferences.

A postdoctoral scientist (2.4 total FTE over the 3-year period) is to be recruited at the Center for Climate Systems Research, Earth Institute, Columbia University. The postdoc will collaborate with the PI to characterize short-term contributions from different cloud types using the different CloudSat-CALIPSO datasets (Activity 1); determine the leading environmental factors of middle- and high-level cloud types and then further document their interannual variation in the observations (Activity 2); and infer their feedbacks using additional reanalysis and global-scale satellite observations (Activity 3). In parallel, the postdoc will apply our framework to the climate models (Activity 4 and 5) and analyze the relationship between cloud feedback and ECS uncertainty in GISS-ModelE3 and CMIP models (Activity 5), besides leading the writing of the related publications and presenting the results in relevant conferences.

Dr. Andrew Ackerman (Co-I, 0.24 total FTE over the 3-year period) is a developer of the GISS model, specialized in cloud-related processes. He will help with the development and implementation of relevant diagnostics in the inline simulators of GISS-ESM to allow a consistent comparison with the observations (Activity 4 and 5) and provide guidance on how to interpret the different results (all activities).

Pr. Helene Chepfer (Collaborator) is an expert on the use of CALIPSO observations for model evaluation and on development of forward simulators with full access to specific outputs of IPSL ESM. She will assist in the comparison of the OPAQ-related simulator diagnostics with CALIPSO-GOCCP OPAQ and provide the OPAQ-related simulator outputs of IPSL ESM for Activity 4 and 5, which are not available on the ESGF database.

Dr. Ann Fridlind (Collaborator) is an expert on mixed-phase and ice-containing clouds. She will provide guidance on how to interpret the different results involving the extratropical clouds, more specifically how changes in cloud parameters related to microphysical processes may affect clouds.

Dr. Maxwell Kelley (Collaborator) is one of the lead developers of the NASA-GISS ESM. He will provide guidance on modifications of all the parameterizations and the physics in the model, as well as in interpretation of results.

Dr. Thibault Vaillant de Guélis (Collaborator) is an expert on the use of CALIPSO observations to understand longwave cloud radiative effect (LW CRE) and to derive associated cloud feedbacks. He will provide guidance on how to use of CALIPSO LW CRE and estimate the different components of the CALIPSO-based LW cloud feedback.

All the members of the proposal team will collaborate with PI Cesana in the writing of the related publications.

4.3. Accomplishments under previous support

Over the past few years, PI Cesana and co-I Ackerman have proven their capabilities in using and developing innovative techniques to exploit CloudSat-CALIPSO observations and climate model outputs to advance understanding of cloud-radiation interactions and cloud feedbacks. Below is a summary of their achievements relevant to the solicitation under previous support.

4.3.1. Expertise in using CALIPSO level1 and CloudSat-CALIPSO level2B datasets to discriminate cloud types and study cloud-radiation interactions

Vertical structure of cloud-radiation interactions. Using the combined CloudSat-CALIPSO 2B-FLXHR-LIDAR radiative-fluxes and CloudSat-CALIPSO 2B-GeoProf level2B observations, Cesana et al. (2019c) assessed the vertical structure of radiative heating rates (RHR) in climate models. In this first-of-its-kind study, they found that the models systematically fail to reproduce observed profiles of cloud RHR. The simulated clouds produce too little warming in the lowest levels compared to the observations, particularly in the tropics.

Discriminating stratocumulus and shallow cumulus clouds. Using CALIPSO level1 and CloudSat-CALIPSO level2B observations, Cesana et al. (2019b) created a dataset, called the Cumulus and Stratocumulus CloudSat-CALIPSO Dataset, to accurately and robustly discriminate stratocumulus and cumulus cloud regimes based on their morphology. Among other findings, their results show that cumulus and stratocumulus are geographically separated more distinctly than suggested by previous satellite data products.

4.3.2. Constraining interannual variations of clouds and cloud feedbacks in ESMs

Inferring Sc and Cu cloud feedback from observations. Building on the CASCCAD dataset, Cesana and Del Genio (2021) estimated observational Sc and Cu cloud feedbacks (using NASA CloudSat-CALIPSO satellite observations) for the first time. They found that Sc drive most of the low-altitude cloud feedback, strong- and weak-warming models are unrealistic and that if current trends of surface warming persist, future warming will be more moderate than many climate models predict.

Evaluating the interannual variability of low clouds in ESMs. Cesana et al. (2019a) studied the interannual variability of low clouds in the GISS models and 12 CMIP5 models, as a function of their ability to represent the interannual vertical structure of the clouds against CALIPSO observations. Their findings show that the models that satisfy the observational constraint are those that represent moist processes within the planetary boundary layer and best capture the observed decrease of low clouds with warming.

Constraining middle- and high-level cloud feedback. Cesana et al. (2021a) showed that including frozen precipitation (stratiform snow) in comparison with CALIPSO measurements and in model radiation schemes is essential to faithfully constrain cloud amount and phase partitioning, and simulate cloud feedbacks. Their findings suggest that making radiation schemes precipitation-aware (missing in most CMIP6 models) should strengthen their positive cloud feedback and further increase their already high mean climate sensitivity.

References

Andrews, T., Gregory, J. M., Webb, M. J. and Taylor, K. E.: Forcing, feedbacks and climate sensitivity in CMIP5 coupled atmosphere-ocean climate models, Geophys. Res. Lett., 39(9), 1–7, doi:10.1029/2012GL051607, 2012.

Bony, S. and Dufresne, J. L.: Marine boundary layer clouds at the heart of tropical cloud feedback uncertainties in climate models, Geophys. Res. Lett., 32(20), L20806, doi:10.1029/2005GL023851, 2005.

Bony, S., Stevens, B., Coppin, D., Becker, T., Reed, K. A., Voigt, A. and Medeiros, B.: Thermodynamic control of anvil cloud amount, Proc. Natl. Acad. Sci. U. S. A., 113(32), 8927–8932, doi:10.1073/pnas.1601472113, 2016.

Bretherton, C. S.: Insights into low-latitude cloud feedbacks from high-resolution models, Philos. Trans. R. Soc. A Math. Phys. Eng. Sci., 373(2054), doi:10.1098/rsta.2014.0415, 2015.

Caldwell, P. M., Zelinka, M. D., Taylor, K. E. and Marvel, K.: Quantifying the sources of intermodel spread in equilibrium climate sensitivity, J. Clim., 29(2), 513–524, doi:10.1175/JCLI-D-15-0352.1, 2016.

Ceppi, P., Brient, F., Zelinka, M. D. and Hartmann, D. L.: Cloud feedback mechanisms and their representation in global climate models, Wiley Interdiscip. Rev. Clim. Chang., 8(4), doi:10.1002/wcc.465, 2017.

Cesana, G. and Chepfer, H.: Evaluation of the cloud thermodynamic phase in a climate model using CALIPSO-GOCCP, J. Geophys. Res. Atmos., 118(14), 7922–7937, doi:10.1002/jgrd.50376, 2013.

Cesana, G., Suselj, K. and Brient, F.: On the Dependence of Cloud Feedbacks on Physical Parameterizations in WRF Aquaplanet Simulations, Geophys. Res. Lett., 44(20), 10,762-10,771, doi:10.1002/2017GL074820, 2017.

Cesana, G., Del Genio, A. D., Ackerman, A. S., Kelley, M., Elsaesser, G., Fridlind, A. M., Cheng, Y. and Yao, M.-S.: Evaluating models' response of tropical low clouds to SST forcings using CALIPSO observations, Atmos. Chem. Phys., 19(5), 2813–2832, doi:10.5194/acp-19-2813-2019, 2019a.

Cesana, G., Del Genio, A. D. and Chepfer, H.: The Cumulus And Stratocumulus CloudSat-CALIPSO Dataset (CASCCAD), Earth Syst. Sci. Data Discuss., 2667637(November), 1–33, doi:10.5194/essd-2019-73, 2019b.

Cesana, G., Waliser, D. E., Henderson, D., L'Ecuyer, T. S., Jiang, X. and Li, J.-L. F.: The Vertical Structure of Radiative Heating Rates: A Multimodel Evaluation Using A-Train Satellite Observations, J. Clim., 32(5), 1573–1590, doi:10.1175/JCLI-D-17-0136.1, 2019c.

Cesana, G. V. and Del Genio, A. D.: Observational constraint on cloud feedbacks suggests moderate climate sensitivity, Nat. Clim. Chang., 11(3), 213–218, doi:10.1038/s41558-020-00970-y, 2021.

Cesana, G.V., A.S. Ackerman, A.M. Fridlind, I. Silber, and M. Kelley: Snow reconciles observed and simulated phase partitioning and doubles cloud feedback in GISS-ModelE3. Geophys. Res. Lett., in review, 2021a.

Cesana, G.V., A.S. Ackerman, T. Vaillant de Guélis, and D. S. Henderson: Cloud-radiation interactions and cloud-climate feedbacks from an active-sensor satellite perspective, in *Climate Impacts of Clouds: Radiation, Circulation, and Precipitation*, S. Sullivan and C. Hoose, *AGU books*, in review, 2021b.

Gregory, J. M., Ingram, W. J., Palmer, M. A., Jones, G. S., Stott, P. A., Thorpe, R. B., Lowe, J. A., Johns, T. C. and Williams, K. D.: A new method for diagnosing radiative forcing and

climate sensitivity, Geophys. Res. Lett., 31(3), 2–5, doi:10.1029/2003GL018747, 2004.
Guzman, R., Chepfer, H., Noel, V., de Guélis, T. V., Kay, J. E., Raberanto, P., Cesana, G., Vaughan, M. A. and Winker, D. M.: Direct atmosphere opacity observations from CALIPSO provide new constraints on cloud-radiation interactions, J. Geophys. Res., 122(2), 1066–1085, doi:10.1002/2016JD025946, 2017.
Hang, Y., L'Ecuyer, T. S., Henderson, D. S., Matus, A. V. and Wang, Z.: Reassessing the effect of cloud type on earth's energy balance in the age of active spaceborne observations. Part II: Atmospheric heating, J. Clim., 32(19), 6219–6236, doi:10.1175/JCLI-D-18-0754.1, 2019.
Hartmann, D. L. and Larson, K.: An important constraint on tropical cloud - climate feedback, Geophys. Res. Lett., 29(20), 12-1-12–4, doi:10.1029/2002gl015835, 2002.
Henderson, D. S., L'ecuyer, T., Stephens, G., Partain, P. and Sekiguchi, M.: A multisensor perspective on the radiative impacts of clouds and aerosols, J. Appl. Meteorol. Climatol., 52(4), 853–871, doi:10.1175/JAMC-D-12-025.1, 2013.
Hourdin, F., Mauritsen, T., Gettelman, A., Golaz, J. C., Balaji, V., Duan, Q., Folini, D., Ji, D., Klocke, D., Qian, Y., Rauser, F., Rio, C., Tomassini, L., Watanabe, M. and Williamson, D.: The art and science of climate model tuning, Bull. Am. Meteorol. Soc., 98(3), 589–602, doi:10.1175/BAMS-D-15-00135.1, 2017.
Kato, S., Rose, F. G., Sun-Mack, S., Miller, W. F., Chen, Y., Rutan, D. A., Stephens, G. L., Loeb, N. G., Minnis, P., Wielicki, B. A., Winker, D. M., Charlock, T. P., Stackhouse, P. W., Xu, K. M. and Collins, W. D.: Improvements of top-of-atmosphere and surface irradiance computations with CALIPSO-, CloudSat-, and MODIS-derived cloud and aerosol properties, J. Geophys. Res. Atmos., 116(19), 1–21, doi:10.1029/2011JD016050, 2011.
Klein, S. A. and Hall, A.: Emergent Constraints for Cloud Feedbacks, Curr. Clim. Chang. Reports, 1(4), 276–287, doi:10.1007/s40641-015-0027-1, 2015.
Klein, S. A., Hall, A., Norris, J. R. and Pincus, R.: Low-Cloud Feedbacks from Cloud-Controlling Factors: A Review, Surv. Geophys., 38(6), 1307–1329, doi:10.1007/s10712-017-9433-3, 2017.
L'Ecuyer, T. S., Hang, Y., Matus, A. V. and Wang, Z.: Reassessing the effect of cloud type on earth's energy balance in the age of active spaceborne observations. Part I: Top of atmosphere and surface, J. Clim., 32(19), 6197–6217, doi:10.1175/JCLI-D-18-0753.1, 2019.
Lenssen, N. J. L., Schmidt, G. A., Hansen, J. E., Menne, M. J., Persin, A., Ruedy, R. and Zyss, D.: Improvements in the GISTEMP Uncertainty Model, J. Geophys. Res. Atmos., 124(12), 6307–6326, doi:10.1029/2018JD029522, 2019.
Loeb, N. G., Doelling, D. R., Wang, H., Su, W., Nguyen, C., Corbett, J. G., Liang, L., Mitrescu, C., Rose, F. G. and Kato, S.: Clouds and the Earth'S Radiant Energy System (CERES) Energy Balanced and Filled (EBAF) top-of-atmosphere (TOA) edition-4.0 data product, J. Clim., 31(2), 895–918, doi:10.1175/JCLI-D-17-0208.1, 2018.
Martins, E., Noel, V. and Chepfer, H.: Properties of cirrus and subvisible cirrus from nighttime Cloud-Aerosol Lidar with Orthogonal Polarization (CALIOP), related to atmospheric dynamics and water vapor, J. Geophys. Res. Atmos., 116(2), 1–19, doi:10.1029/2010JD014519, 2011.
Matus, A. V. and L'Ecuyer, T. S.: The role of cloud phase in Earth's radiation budget, J. Geophys. Res., 122(5), 2559–2578, doi:10.1002/2016JD025951, 2017.
McCoy, D. T., Eastman, R., Hartmann, D. L. and Wood, R.: The change in low cloud cover in a warmed climate inferred from AIRS, MODIS, and ERA-interim, J. Clim., 30(10), 3609–3620, doi:10.1175/JCLI-D-15-0734.1, 2017.

Morice, C. P., Kennedy, J. J., Rayner, N. A. and Jones, P. D.: Quantifying uncertainties in global and regional temperature change using an ensemble of observational estimates: The HadCRUT4 data set, J. Geophys. Res. Atmos., 117(8), 1–22, doi:10.1029/2011JD017187, 2012.
Myers, T. A. and Norris, J. R.: On the relationships between subtropical clouds and meteorology in observations and CMIP3 and CMIP5 models, J. Clim., 28(8), 2945–2967, doi:10.1175/JCLI-D-14-00475.1, 2015.
Myers, T. A. and Norris, J. R.: Reducing the uncertainty in subtropical cloud feedback, Geophys. Res. Lett., 43(5), 2144–2148, doi:10.1002/2015GL067416, 2016.
Myers, T. A., Mechoso, C. R., Cesana, G. V., DeFlorio, M. J. and Waliser, D. E.: Cloud Feedback Key to Marine Heatwave off Baja California, Geophys. Res. Lett., 45(9), 4345–4352, doi:10.1029/2018GL078242, 2018.
Myers, T. A., Scott, R. C., Zelinka, M. D., Klein, S. A., Norris, J. R. and Caldwell, P. M.: Observational constraints on low cloud feedback reduce uncertainty of climate sensitivity, Nat. Clim. Chang., 11(6), 501–507, doi:10.1038/s41558-021-01039-0, 2021.
Qu, X., Hall, A., Klein, S. A. and Caldwell, P. M.: On the spread of changes in marine low cloud cover in climate model simulations of the 21st century, Clim. Dyn., 42(9–10), 2603–2626, doi:10.1007/s00382-013-1945-z, 2014.
Qu, X., Hall, A., Klein, S. A. and Deangelis, A. M.: Positive tropical marine low-cloud cover feedback inferred from cloud-controlling factors, Geophys. Res. Lett., 42(18), 7767–7775, doi:10.1002/2015GL065627, 2015.
Qu, X., Hall, A., DeAngelis, A. M., Zelinka, M. D., Klein, S. A., Su, H., Tian, B. and Zhai, C.: On the emergent constraints of climate sensitivity, J. Clim., 31(2), 863–875, doi:10.1175/JCLI-D-17-0482.1, 2018.
Rohde, R. and Hausfather, Z.: The Berkeley Earth Land/Ocean Temperature Record, Earth Syst. Sci. Data Discuss., 4, 1–16, doi:10.5194/essd-2019-259, 2020.
Saint-Lu, M., Bony, S. and Dufresne, J. L.: Observational Evidence for a Stability Iris Effect in the Tropics, Geophys. Res. Lett., 47(14), doi:10.1029/2020GL089059, 2020.
Sassen, K. and Wang, Z.: Classifying clouds around the globe with the CloudSat radar : 1-year of results, , 35(January), 1–5, doi:10.1029/2007GL032591, 2008.
Schiro, K. A., Sullivan, S. C., Kuo, Y. H., Su, H., Gentine, P., Elsaesser, G. S., Jiang, J. H. and Neelin, J. D.: Environmental controls on tropical mesoscale convective system precipitation intensity, J. Atmos. Sci., 77(12), 4233–4249, doi:10.1175/JAS-D-20-0111.1, 2020.
Scott, R. C., Myers, T. A., Norris, J. R., Zelinka, M. D., Klein, S. A., Sun, M. and Doelling, D. R.: Observed sensitivity of low-cloud radiative effects to meteorological perturbations over the global oceans, J. Clim., 33(18), 7717–7734, doi:10.1175/JCLI-D-19-1028.1, 2020.
Sherwood, S. C., Webb, M. J., Annan, J. D., Armour, K. C., Forster, P. M., Hargreaves, J. C., Hegerl, G., Klein, S. A., Marvel, K. D., Rohling, E. J., Watanabe, M., Andrews, T., Braconnot, P., Bretherton, C. S., Foster, G. L., Hausfather, Z., von der Heydt, A. S., Knutti, R., Mauritsen, T., Norris, J. R., Proistosescu, C., Rugenstein, M., Schmidt, G. A., Tokarska, K. B. and Zelinka, M. D.: An Assessment of Earth's Climate Sensitivity Using Multiple Lines of Evidence, Rev. Geophys., 58(4), 1–92, doi:10.1029/2019RG000678, 2020.
Su, H., Jiang, J. H., Zhai, C., Shen, T. J., Neelin, J. D., Stephens, G. L. and Yung, Y.: Weakening and strengthening structures in the hadley circulation and the implications for climate sensitivity, J. Geophys. Res. Atmos., 119, 5787–5805, doi:10.1002/2014JD021642.Received, 2014.

Terai, C. R., Klein, S. A. and Zelinka, M. D.: Constraining the low-cloud optical depth feedback at middle and high latitudes using satellite observations, J. Geophys. Res., 121(16), 9696–9716, doi:10.1002/2016JD025233, 2016.

Vaillant de Guélis, T., Chepfer, H., Guzman, R., Bonazzola, M., Winker, D. M. and Noel, V.: Space lidar observations constrain longwave cloud feedback, Sci. Rep., 8(1), 16570, doi:10.1038/s41598-018-34943-1, 2018.

Vial, J., Dufresne, J. L. and Bony, S.: On the interpretation of inter-model spread in CMIP5 climate sensitivity estimates, Clim. Dyn., 41(11–12), 3339–3362, doi:10.1007/s00382-013-1725-9, 2013.

Zelinka, M. D. and Hartmann, D. L.: Why is longwave cloud feedback positive?, J. Geophys. Res. Atmos., 115(16), 1–16, doi:10.1029/2010JD013817, 2010.

Zelinka, M. D. and Hartmann, D. L.: The observed sensitivity of high clouds to mean surface temperature anomalies in the tropics, J. Geophys. Res. Atmos., 116(23), 1–16, doi:10.1029/2011JD016459, 2011.

Zelinka, M. D., Klein, S. A., Taylor, K. E., Andrews, T., Webb, M. J., Gregory, J. M. and Forster, P. M.: Contributions of different cloud types to feedbacks and rapid adjustments in CMIP5, J. Clim., 26(14), 5007–5027, doi:10.1175/JCLI-D-12-00555.1, 2013.

Zelinka, M. D., Zhou, C. and Klein, S. A.: Insights from a refined decomposition of cloud feedbacks, Geophys. Res. Lett., 43(17), 9259–9269, doi:10.1002/2016GL069917, 2016.

Zelinka, M. D., Randall, D. A., Webb, M. J. and Klein, S. A.: Clearing clouds of uncertainty, Nat. Clim. Chang., 7(10), 674–678, doi:10.1038/nclimate3402, 2017.

Zelinka, M. D., Myers, T. A., McCoy, D. T., Po-Chedley, S., Caldwell, P. M., Ceppi, P., Klein, S. A. and Taylor, K. E.: Causes of Higher Climate Sensitivity in CMIP6 Models, Geophys. Res. Lett., 47(1), 1–12, doi:10.1029/2019GL085782, 2020.

Zhai, C., Jiang, J. H. and Su, H.: Long-term cloud change imprinted in seasonal cloud variation: More evidence of high climate sensitivity, Geophys. Res. Lett., 42(20), 8729–8737, doi:10.1002/2015GL065911, 2015.